

## **T2WELL—AN INTEGRATED WELLBORE-RESERVOIR SIMULATOR**

Lehua Pan and Curtis M. Oldenburg

Earth Sciences Division 74-316C  
Lawrence Berkeley National Laboratory  
Berkeley, CA 94720, USA  
e-mail: lpan@lbl.gov, cmoldenburg@lbl.gov

### **ABSTRACT**

We have developed T2Well, a numerical simulator for nonisothermal, multiphase, multicomponent flows in integrated wellbore-reservoir systems. The new model extends the existing numerical reservoir simulator TOUGH2 to calculate the flow in both the wellbore and the reservoir simultaneously and efficiently, by introducing a special wellbore subdomain into the numerical grid. For gridblocks in the wellbore subdomain, we solve the 1D momentum equation of the mixture (which may be two-phase) as described by the Drift-Flux Model (DFM). The velocity of the mixture is calculated by solving the momentum equation numerically, while the individual phase velocities are calculated from the mixture velocity and other fluid parameters as defined by the DFM. A novel mixed implicit-explicit scheme is applied to facilitate the solution of the momentum equation within the Newton-Raphson iteration framework of TOUGH2. Specifically, the pressure gradient, gravity component, and time derivative of momentum are treated fully implicitly, whereas the spatial gradient of momentum is treated explicitly. The friction term is calculated with a mixed implicit-explicit scheme. Applications of the new simulator to problems in various fields are presented to demonstrate its capabilities.

### **INTRODUCTION**

At its most basic level, management of subsurface resources involves a system comprising the wellbore and the target reservoir. As discrete pathways through geologic formations, boreholes and wells are critical to the success of many water, energy, and environmental management operations (e.g., geologic carbon sequestration, oil and gas production, compressed air energy storage, geothermal energy production, and subsurface remediation).

Simulating nonisothermal, multiphase, and multicomponent flows in both wellbore and reservoir as an integrated system (as it is in reality) remains a challenging, yet important task, required to answer critical questions as to the design and performance of fluid production, injection, and transport systems.

Because of the many water, energy, and environmental applications of wellbore-reservoir systems, many stand-alone simulators have been developed for two-phase flow in wellbores with various levels of coupling to the reservoir, even though the flow processes in wellbores and in reservoirs are often strongly coupled in reality. Lu and Connell (2008) proposed a quasi-steady numerical approach that included two-phase flow of CO<sub>2</sub> and used a productivity index approach to couple the wellbore to the reservoir. Lindeberg (2011) included transient effects of two-phase CO<sub>2</sub> flows in the well without coupling to the reservoir. Remoroza et al. (2011) developed an approach for geothermal applications that coupled the wellbore flow with the reservoir, but assumed steady-state and single-phase flow in the well. Hadgu et al. (1995) developed a similar approach for geothermal applications using dynamic production index methods. Livescu et al. (2009) developed fully coupled wellbore-reservoir flow simulators for oil/gas industry applications, using a simplified correction term to account for the transient flow in the wellbore.

The main difficulties for simulating wellbore-reservoir flow as an integrated system are the following: (1) different governing equations apply to the wellbore and the reservoir that need to be solved efficiently in a uniform framework; (2) the significant contrast in temporal and spatial scale between the wellbore and the reservoir that results in a very challenging set of stiff

partial differential equations, and (3) other complexities (e.g., dryout) that are caused by the interactions between the wellbore and the reservoir.

This paper presents a new approach that we recently developed for simulating non-isothermal, two-phase, multicomponent flow in a wellbore-reservoir system. The new model (T2Well) uses an integrated wellbore-reservoir system in which the wellbore and reservoir are two different subdomains in which flow is controlled by different physics, but solved uniformly within the Newton-Raphson iteration scheme in the TOUGH2 code.

## THEORY

We treat the wellbore-reservoir flow problem as an integrated system in which the wellbore and reservoir are two different subdomains, within which flow is controlled by different physics—specifically, viscous flow in the wellbore is governed by the 1D momentum equation, and 3D flow through porous media in the reservoir is governed by a multiphase version of Darcy's law. As a result, the governing equations for the flow processes in a wellbore-reservoir system are an extended set of those used by the standard TOUGH2. As shown in Table 1, the major differences in governing equations between the wellbore and the reservoir are the definitions of energy flow terms and the phase velocities. Because the velocities in the reservoir are usually very small, the kinetic energy can be ignored in the energy balance, and the phase velocities can be calculated by the multiphase Darcy's law.

However, this is not the case in the wellbore, where the kinetic energy cannot be ignored and the phase velocities are governed by two-phase momentum equations. Even though the wellbore flow can be reasonably simplified as 1D, the two-phase momentum equations are still very difficult to solve, mainly because of the complex two-phase flow structure in wellbores. The Drift-Flux-Model (DFM), first developed by Zuber and Findlay (1965) and Wallis (1969), among others, provides a conceptually robust and simpler way to tackle the problem.

Table 1. The mass and energy balance equations solved in T2Well

Description	Equation
Conservation of mass and energy	$\frac{d}{dt} \int_{V_n} M^\kappa dV_n = \int_{\Gamma_n} \mathbf{F}^\kappa \cdot \mathbf{n} d\Gamma_n + \int_{V_n} q^\kappa dV_n$
Mass accumulation	$M^\kappa = \phi \sum_\beta S_\beta \rho_\beta X_\beta^\kappa$ for each mass component
Mass flux	$\mathbf{F}^\kappa = \sum_\beta X_\beta^\kappa \rho_\beta \mathbf{u}_\beta$ for each mass component
Energy flux	$\mathbf{F}^\kappa = -\lambda \nabla T + \sum_\beta h_\beta \rho_\beta \mathbf{u}_\beta$
Porous media Energy accumulation	$M^\kappa = (1 - \varphi) \rho_R C_R T + \varphi \sum_\beta \rho_\beta S_\beta U_\beta$
Phase velocity	$\mathbf{u}_\beta = -k \frac{k_{r\beta}}{\mu_\beta} (\nabla P_\beta - \rho_\beta \mathbf{g})$
Energy flux	$F^\kappa = -\lambda \frac{\partial T}{\partial z} - \frac{1}{A} \sum_\beta \frac{\partial}{\partial z} \left( A \rho_\beta S_\beta u_\beta \left( h_\beta + \frac{u_\beta^2}{2} \right) \right) - \sum_\beta (S_\beta \rho_\beta u_\beta g \cos \theta) - q''$
Energy accumulation	$M^\kappa = \sum_\beta \rho_\beta S_\beta \left( U_\beta + \frac{1}{2} u_\beta^2 \right)$
Wellbore Phase velocity	$u_G = C_0 \frac{\rho_m}{\rho_m^*} u_m + \frac{\rho_L}{\rho_m^*} u_d$ $u_L = \frac{(1 - S_G C_0) \rho_m}{(1 - S_G) \rho_m^*} u_m - \frac{S_G \rho_G}{(1 - S_G) \rho_m^*} u_d$

Although various nomenclatures and forms of equations have been used in the literature over the recent past to describe DFM approach, its the basic idea is to assume that the gas velocity,  $u_G$ , can be related to the volumetric flux of the mixture,  $j$ , and the drift velocity of gas,  $u_d$ , by the empirical constitutive relationship:

$$u_G = C_0 j + u_d \quad (1)$$

where  $C_0$  is the profile parameter to account for the effect of local gas saturation and velocity profiles over the pipe cross-section. The liquid velocity  $u_L$  can be solved by considering the definition of the volumetric flux of the mixture

$$u_L = \frac{1 - S_G C_0}{1 - S_G} j - \frac{S_G}{1 - S_G} u_d \quad (2).$$

where  $S_G$  is the gas phase saturation.

With the drift-flux model (1)-(2), the momentum equations of two-phase flow in a wellbore can be simplified into a single equation in terms of the mixture velocity  $u_m$  and the drift velocity  $u_d$  as follows (Pan et al., 2011a, Appendix A):

$$\frac{\partial}{\partial t}(\rho_m u_m) + \frac{1}{A} \frac{\partial}{\partial z} [A(\rho_m u_m^2 + \gamma)] = -\frac{\partial P}{\partial z} - \frac{\Gamma f \rho_m |u_m| u_m}{2A} - \rho_m g \cos \theta \quad (3)$$

where the term

$$\gamma = \frac{S_G}{1-S_G} \frac{\rho_G \rho_L \rho_m}{\rho_m^{*2}} [(C_0 - 1)u_m + u_d]^2 \quad \text{is}$$

caused by slip between the two phases. The terms  $\rho_m$ ,  $u_m$ , and  $\rho_m^*$  are the mixture density, the mixture velocity (mass centered), and the profile-adjusted average density of the mixture.

Therefore, with the DFM approach, solving the complicated momentum equations of two-phase flow becomes an easier task executed in two steps. First, we obtain the mixture velocity by solving the momentum equation (3) and the drift velocity from empirical relationships (discussed below). Second, we calculate the gas velocity and the liquid velocity as a function of  $u_m$  and  $u_d$ .

The empirical relationships for the drift velocity and the profile parameter used in T2Well/ECO2N are based on the drift flux model developed by Shi et al. (2005). They proposed functional forms for the profile parameter and drift velocity with a set of optimized parameters obtained from an extensive set of large-scale pipe flow experiments performed by Oddie et al. (2003) for one-, two-, and three-phase flow at various inclinations. These functional forms can be applied continuously for all flow regimes, from bubble flow to film flow. A summary of the mathematical formulations related to the drift velocity proposed by Shi et al. (2005) that are implemented in T2Well can be found in the T2Well/ECO2N manual (Pan et al., 2011c) and a related paper (Pan et al., 2011b).

Because the original equation for drift velocity proposed by Shi et al. (2005) cannot be applied to the mist flow regime, i.e., the special two-phase flow pattern that often occurs at high velocity and high gas mass fraction,  $X$ . In the mist flow regime, the gas velocity is so high that the small amount of liquid (i.e.,  $X \approx 1$ ) cannot form a film, but instead forms tiny droplets that are uniformly distributed in the gas flow. As a result, the slip between the two phases in the mist flow regime diminishes. Cheng et al. (2008)

developed a flow pattern map for CO<sub>2</sub> that suggests that the mist flow regime occurs when mass velocity (i.e., the total mass flow rate per unit cross-sectional area,  $G$ ) reaches more than 300 kg/m<sup>2</sup>/s at higher  $X$ . To account for this region, we used a modified equation to calculate the drift velocity as follows:

$$u_d = \frac{(1 - S_G) u_c K(S_G, K_u) m(\theta) f(G, X)}{S_G \sqrt{\rho_G / \rho_L} + 1 - S_G} \quad (4).$$

The adjustment function  $f(G, X)$  is a smooth function that quickly approaches zero as the state point in the  $G$ - $X$  plane approaches the mist flow regime, whereas it would equal one everywhere else (Pan et al., 2011a, Appendix B). In addition, a cosine-type function  $K(\bullet)$  is used in (4) to make a smooth transition of drift velocity between the bubble-rise stage and the film-flooding stage, which is slightly different from the linear interpolation suggested by Shi et al. (2005).

## IMPLEMENTATION

The component mass- and energy-balance equations of Table 1 are discretized in space using the conventional integrated finite-difference scheme of TOUGH2 for both the wellbore and the reservoir. Apart from the special treatment of the momentum equation for wellbore (discussed below), time discretization is carried out using a backward, first-order, fully implicit finite-difference scheme. In the framework of TOUGH2, the discretized mass and energy conservation equations are written in residual forms as functions of primary variables, and are solved using Newton-Raphson iteration, during which all elements in the Jacobian matrix are evaluated by numerical differentiation (Pruess et al., 1999).

Unlike in the reservoir, where the phase velocities can simply be obtained using Darcy's Law, the phase velocities in the wellbore are functions of the mixture velocity, which is an unknown variable of the momentum equation. Solving an additional governing equation (i.e., the momentum equation) simultaneously is tedious, because (1) the momentum equation is only needed for a

very small portion of the domain (i.e., the wellbore) and (2) the velocity is naturally defined at the interfaces between grid cells, whereas other primary variables are defined at the grid cells. Our approach is to solve the momentum equation using a hybrid formula at interfaces of the neighboring wellbore cells as

$$u_m^{n+1} = \frac{DR^{n+1} + \frac{1}{\Delta t} \rho_m^n u_m^n - \left( \frac{1}{A} \frac{\partial}{\partial z} \left( A \sum_p \rho_p S_p u_p^2 \right) \right)^n}{\frac{\rho_m^{n+1}}{\Delta t} + \frac{f^n \Gamma \rho_m^{n+1} |u_m^n|}{2A}} \quad (5)$$

where, the superscripts  $n$  and  $n + 1$  indicate the previous and current time levels, respectively;  $\Delta t$  is the time-step size, and  $DR$  is the total driving force given by

$$DR = -\frac{\partial P}{\partial z} - \rho_m g \cos \theta \quad (6).$$

Here, the driving force term (pressure gradient and gravity) is treated fully implicitly, whereas the spatial acceleration term is treated explicitly. The friction term is evaluated part explicitly and part implicitly.

The flow terms at the interface between the perforated wellbore sections and the surrounding formations are calculated based on Darcy's law, because they are usually limited by the flow through formations. However, the nodal distance to the interface of the wellbore side is set to zero, which is equivalent to the resistance to flow inside the wellbore being negligible relative to that on the formation side.

The heat exchanges between wellbore and the surrounding formation will either be calculated as the "normal" heat flow terms in standard TOUGH2, if the surrounding formation is explicitly represented in the numerical grid, or they will be calculated (optionally) semi-analytically (Ramey, 1962), if no gridblocks of the surrounding formation exist.

In standard TOUGH2, besides pressure, temperature, and gas saturation (if two phase), the mass fractions of non-water components are usually used as the primary variables. However, this practice could be problematic for a system with multiple gas components (e.g.,  $\text{CO}_2$ ,  $\text{CH}_4$ , and air), especially if one or more of the components disappear at any cells in the domain. This is

because physically, the sum of all mass fractions should be one at all gridblocks. As a result, the partial derivative with respect to one mass component could become close to a linear function of the partial derivative with respect to another mass component, especially if one of the three mass components does not exist. Consequently, the Jacobian matrix would become singular or close to singular, resulting in a failure of the Newton-Raphson iteration. To avoid this trouble, a new set of primary variables (for the gas components) is used. Taking the research module EOS7CMA (water, brine,  $\text{CO}_2$ ,  $\text{CH}_4$ , air) as an example, the new primary variables  $X_3$  and  $X_4$  are defined as the scaled mass fraction in noncondensable mass components, as follows:

$$X_3 = \frac{2X_{\text{CO}_2}}{X_{\text{CO}_2} + X_{nc}} \quad (7a)$$

$$X_4 = \frac{2X_{\text{CH}_4}}{X_{\text{CH}_4} + X_{nc}} \quad (7b)$$

$$X_5 = \begin{cases} S_g & \text{if two-phase} \\ X_{nc} & \text{otherwise} \end{cases} \quad (7c)$$

where  $X_{nc}$  is the total mass fraction of non-condensable gas components ( $= X_{\text{CO}_2} + X_{\text{CH}_4} + X_{\text{air}}$ ). Each mass component can be easily calculated from the primary variables as follows:

$$X_{\text{CO}_2} = \frac{X_3 X_{nc}}{2 - X_3} \quad (8a)$$

$$X_{\text{CH}_4} = \frac{X_4 X_{nc}}{2 - X_4} \quad (8b)$$

$$X_{\text{air}} = X_{nc} - X_{\text{CO}_2} - X_{\text{CH}_4} \quad (8c)$$

In the case of two-phase conditions,  $X_{nc}$  is obtained by solving the solubility equation in a similar way as in standard TOUGH2. The new primary variables defined in (7) would never be co-linear. However, numerical differentiation could still lead to negative mass fraction, which could either cause problems in the calculation of fluid properties if not forced to zero, or worsen the condition of the Jacobian matrix if forced to zero, for the case in which the air component does not exist or only  $\text{CO}_2$  or  $\text{CH}_4$  exists in any gridblock. In this case, a special formula for

calculating the increments in primary variables ( $X_3$  and  $X_4$ ) is used to enforce that all mass fractions be in physically reasonable ranges and that Equation (8c) is conserved such that the partial derivatives with respect to each primary variable are not linearly correlated.

## VERIFICATION AND APPLICATION EXAMPLES

### Verification against an analytical solution of steady-state two-phase flow

To verify the T2Well code, we first compare the numerical model against the analytical solution by Pan et al. (2011a). We consider an idealized problem of steady-state, isothermal, two-phase (air and water) flow through a vertical wellbore of 1000 m length.

The T2Well/EOS3 problem is run as a transient problem with adaptive time steps. The ending simulation time is  $7.85 \times 10^8$  seconds (4100 steps), at which the average time-derivative of momentum is about  $-2.2 \times 10^{-17}$  (Pa/m), indicating an effective steady state was reached. As shown in Figure 1, the agreement is very good between the numerical solution and the analytical solution (coefficient of determination  $R^2 > 0.998$ ).

### Validation with field CO<sub>2</sub> production test data

To demonstrate the adequacy of T2Well to describe wellbore flow in an actual well, we compared T2Well/ECO2N simulation results to the field data of Cronshaw and Bolling (1982). Flow in the wellbore was believed to reach steady-state after half a day during a field production test (Cronshaw and Bolling, 1982), and the pressure and temperature data were measured at that time. In total, four flow rates (2.5, 7.4, 11.2, and 13.7 kg/s) were used in the test. The well had a length of 914.4 m with a incline angle of 26.5°. Its diameter was 0.088 m.

In these simulations, only the lower portion (below the measured depth of 595 m) of the wellbore was simulated, because three-phase (water, liquid CO<sub>2</sub>, and gaseous CO<sub>2</sub>) conditions may develop in the upper portion of the wellbore, which is beyond the phase handling capability of

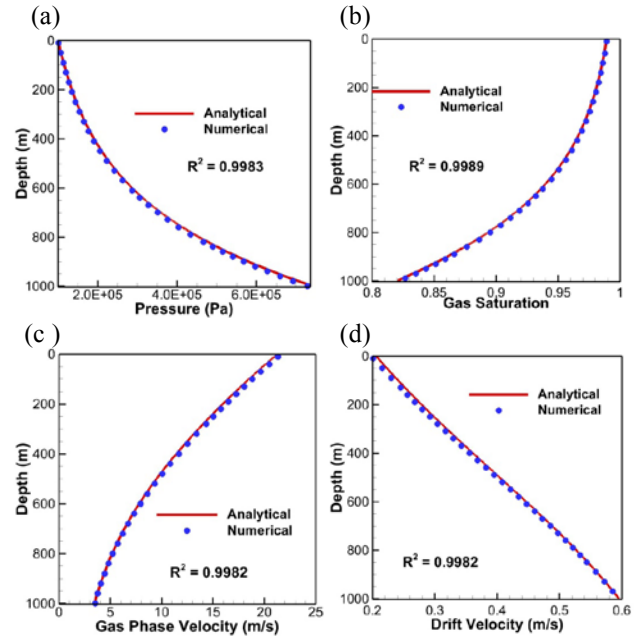


Figure 1. Depth profiles of pressure, gas saturation, gas-phase velocity, and drift velocity under steady-state, isothermal, two-phase (air/water) flow conditions in a vertical wellbore showing excellent agreement between analytical and numerical results.  $R^2$  is the coefficient of determination.

ECO2N. The heat exchange between the wellbore and the surrounding formation is calculated using an analytical approach implemented in the code, and the corresponding heat conductivity is 2.51 (W/m oC). The vertical grid resolution is 1 m.

As shown in Figure 2, the match between the simulated results and the field data is reasonably good, except for the extra-high temperature at the measured depth of 750 m for case R1. Cronshaw and Bolling (1982) did not explain why the measured temperature at that point in Case R1 was higher than the ambient formation temperature and very close to the temperature at 914 m depth. One possibility is that a vertical convective heat-transfer mechanism in the annulus outside the production tube was established prior to the production test, which was able to maintain an almost constant temperature in the well completion fluid up to the depth of 750 m (at least) before production. As a result, the production tube was effectively surrounded by the hot fluid, which enhanced the lateral heat exchange and tended to maintain a higher

temperature in the lower portion of the tube. If this is the case, the density of CO<sub>2</sub> in the production tube would be lower, and thus the gravity-pressure loss would be smaller than that without this additional heating. This temperature difference seems to contribute to the under-predictions of pressure by the model for the lower flow rate cases, because the model does not include this additional heating mechanism. Even when we tried to compensate for this effect by slightly altering the T and P boundary conditions, the predicted pressure profile was still not as steep as the measured ones for cases R1 and R2, mainly because of the overestimation of the density (increasing as temperature decreases) resulting from ignoring such heat exchange effects. Notably, this effect becomes much smaller as the flow rate increases (i.e., the inflow CO<sub>2</sub> becomes more dominant). As a result, the deviations between predictions and the measured data become smaller for the higher flow-rate cases.

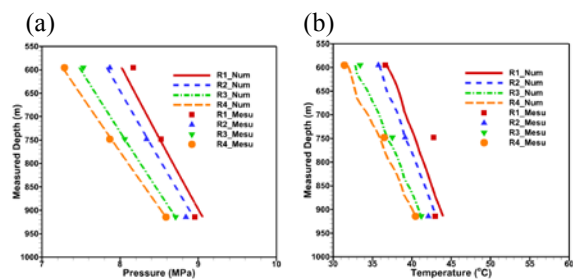


Figure 2. Simulated depth profiles of pressure (a) and temperature (b) after 12 hours of production under different flow rates as compared to the measured data. Lines are predictions by T2Well/ECO2n, and symbols are the measured data (red – R1; blue – R2; green – R3; and yellow – R4).

Cronshaw and Bolling (1982) did not report the downhole gas saturation, but mentioned that their model was able to predict the pressure profile correctly only if assuming pure CO<sub>2</sub> production, even though there was 3% water produced in each case. In our simulations, the gas saturation at well bottom was assigned between 0.988 and 0.989, which was obtained from the previous analytical solutions (Pan et al., 2011a). The predicted water fraction in the produced fluid is 3.16%, 3.06%, 2.99%, and 2.99% for cases R1, R2, R3, and R4, respectively, which are pretty close to the reported value of 3%.

### Estimation of oil and gas flow-rate for the 2010 BP Macondo Well Blowout

On April 20, 2010, the Macondo well drilled by BP from the Deepwater Horizon floating platform in the Gulf of Mexico suffered a blowout. Eleven people were killed by the explosion and fire on the platform shortly after the blowout. Estimation of the magnitude of the oil and gas discharge into the marine environment became an urgent priority after numerous attempts to stem the flow failed. Such an estimate would be critical for addressing the environmental consequences of the oil and gas release, for developing engineering solutions for a temporary containment cap, and for evaluating the liability of the operating companies for the resulting environmental damage.

T2Well was used with a simplified TOUGH2 EOS for oil to estimate the gas and oil flow rate (Oldenburg et al., 2011). The model was constructed as a single well problem in a simple radial symmetric reservoir. Figure 3 shows the oil and gas flow rates for various lengths of opening of the wellbore in the reservoir. In addition to sensitivity of results to the connectivity of the well and the reservoir, we also observed sensitivity of results to the pressure at the bottom of the blowout preventer. This pressure boundary condition also controls the amount of degassing of the oil during upward flow in the well, which in turn affects oil flow rate (Oldenburg et al., 2011).

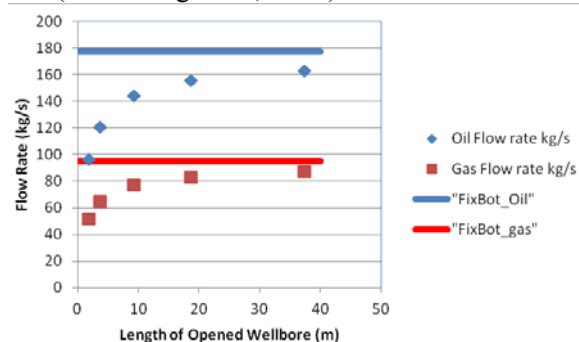


Figure 3. Simulated oil and gas flow rates as response to the length of opened ("broken") wellbore. "FixBot\_oil" and "FixBot\_gas" are the simulated flow rates as if the wellbore is attached to an infinite pool of oil under reservoir conditions (i.e., the upper limit for the given parameters).

### **Modeling brine leakage to shallow aquifer through an open well**

Potential leakage of brine to a shallower potable aquifer through open wellbores is a common concern for GCS projects, because the area of hydraulic overpressure is usually much larger than the free-phase plume, and many wellbores may be completely plugged only near the land surface. T2Well was used to study such a problem (Hu et al., 2011). A hypothetical system consists of two aquifers separated by a thick aquitard but connected by an open wellbore which is closed at the land surface as well as the aquitard formation, but fully perforated in both aquifers (Figure 4(a)). The system starts at hydrostatic conditions with various salinity conditions and responds to a pressure perturbation at the far end of the lower aquifer as if CO<sub>2</sub> were injected into the lower aquifer at a great distance from the well.

Figure 4(b) shows the simulated brine leakage rates 10 days after the pressure perturbation is applied. As expected, the lower the salinity, the higher the leakage rate under the same pressure perturbation, and the leakage rate increases with the pressure perturbation. However, the widely used EDM (Equivalent Darcy Medium) approach could over- or underestimate the leakage rate, depending on specific conditions. The critical equivalent permeability for the wellbore used in the EDM approach is not an intrinsic parameter of the wellbore, but rather a function of flow status, simply because the flow in an open wellbore does not in general obey Darcy's law.

### **CONCLUSION**

We have developed a new modeling approach that can simulate nonisothermal, two-phase, multicomponent flow in wellbores connected to reservoirs as an integrated system within the framework of TOUGH2. The new model has been verified against both analytical solutions and field-measured data gathered during a CO<sub>2</sub> production test. As demonstrated in the example applications, the code can be used to analyze many practical problems in various fields with proper EOS modules. In many cases, the integrated wellbore-reservoir modeling approach is necessary for correctly solving problems that

could not be solved by wellbore or reservoir simulator alone.

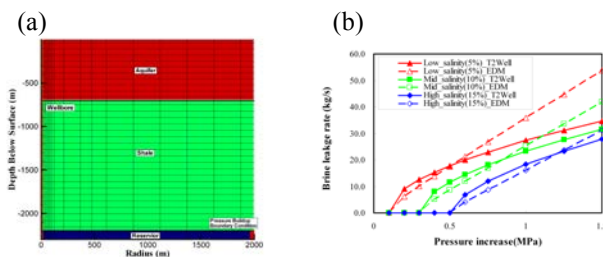


Figure 4. (a) A radial symmetric grid for a two-aquifer, one-aquitard, and one-well system. (b) Simulated leakage rates (after 10 days) as response to the pressure perturbation under the effects of 5%, 10%, and 15% salinity by T2Well and EDM (Equivalent Darcy Medium) approach. The equivalent permeability for the wellbore in the EDM model was obtained by matching the flow rate under the low salinity (5%) case as response to 0.5 MPa pressure perturbation calculated by T2Well.

### **ACKNOWLEDGEMENT**

This work was supported, in part, by the CO<sub>2</sub> Capture Project (CCP) of the Joint Industry Program (JIP), by the National Risk Assessment Partnership (NRAP) through the Assistant Secretary for Fossil Energy, Office of Sequestration, Hydrogen, and Clean Coal Fuels, through the National Energy Technology Laboratory, and by Lawrence Berkeley National Laboratory under U.S. Department of Energy Contract No. DE-AC02-05CH11231.

### **REFERENCES**

- Cheng, L., G. Ribatski, J.M. Quiben, J.R. Thome. New prediction methods for CO<sub>2</sub> evaporation inside tubes: Part I – A two-phase flow pattern map and a flow pattern based phenomenological model for two-phase flow frictional pressure drops, *Int. J Heat and Mass Transfer*, 51: 111–124, 2008.
- Cronshaw, M.B. and J.D. Bolling. A numerical model of the non-isothermal flow of carbon dioxide in wellbores. In: SPE 10735, SPE California Regional Meeting, San Francisco, May 22-26, 1982.



- Hadgu, T., R.W. Zimmerman, and G.S. Bodvarsson. Coupled reservoir-wellbore simulation of geothermal reservoir behavior. *Geothermics* 24(2), 145-166, 1995.
- Hu, L., L. Pan, and K. Zhang. Modeling brine leakage to shallow aquifer through an open wellbore using T2WELL/ECO2N. *International J. of Greenhouse Gas Control*, 9 393–401, 2012.
- Lindeberg, E. Modelling pressure and temperature profile in a CO<sub>2</sub> injection well, *Energy Procedia*, 4, 3935-3941, 2011.
- Livescu, S., L.J. Durlofsky, K. Aziz, and J.C. Ginestra. A fully-coupled thermal multi-phase wellbore flow model for use in reservoir simulation. *J. of Petroleum Science and Engineering*, 2009.
- Lu, M. and L.D. Connell. Non-isothermal Flow of Carbon Dioxide in Injection Wells during Geological Storage, *Int. J. Greenhouse Gas Control*, 2(2), pp. 248–258, 2008.
- Oddie, G., H. Shi, L.J. Durlofsky, K. Aziz, B. Pfeffer, and J.A. Holmes. Experimental study of two and three phase flows in large diameter inclined pipes, *Int. J Multiphase Flow*, 29:527–558, 2003.
- Oldenburg, C.M., B.M. Freifeld, K. Pruess, L. Pan, S.A. Finsterle, and G. Moridis. Numerical simulations of the Macondo well blowout reveal strong control of oil flow by reservoir permeability and exsolution of gas, *Proc. National Acad. Sci.*, Early Edition, 2011.
- Pan L., S.W. Webb, and C.M. Oldenburg. Analytical solution for two-phase flow in a wellbore using the drift-flux model. *Advances in Water Resources*. 34, 1656–1665, 2011a.
- Pan L., C.M. Oldenburg, K. Pruess, and Y.-S. Wu. Transient CO<sub>2</sub> leakage and injection in wellbore-reservoir systems for geologic carbon sequestration. *Greenhouse Gas Sci Technol*. 1:335–350; DOI: 10.1002/ghg, 2011b.
- Pan, L., Y.-S. Wu, C.M. Oldenburg, and K. Pruess. T2Well/ECO2N Version 1.0: Multi-phase and Non-Isothermal Model for Coupled Wellbore-Reservoir Flow of Carbon Dioxide and Variable Salinity Water. LBNL-4291E, 2011c.
- Pruess, K., C.M. Oldenburg, and G.J. Moridis. TOUGH2 User's Guide Version 2. Lawrence Berkeley National Laboratory Report, LBNL-43134, November 1999.
- Ramey Jr, H.J. Wellbore heat transmission. *J. of Petroleum Technology*, 225, 427–435, 1962.
- Remoroza, A.I., B. Moghtaderi, and E. Doroodchi. Coupled wellbore and 3D reservoir simulation of a CO<sub>2</sub> EGS, Proceedings, SGP-TR-191, Thirty-Sixth Workshop on Geothermal Reservoir Engineering, Stanford University, Stanford, California, Jan 31 - Feb 2, 2011.
- Shi, H., J.A. Holmes, L.J. Durlofsky, K. Aziz, L.R. Diaz, B. Alkaya, and G. Oddie. Drift-flux modeling of two-phase flow in wellbores, *Soc. Pet. Eng. J.*, 10(1), 24-33, 2005.
- Wallis, G.B. One-dimensional Two-phase Flow, McGraw-Hill Book Company, New York, 1969.
- Zuber, N. and J.A. Findlay. Average volumetric concentration in two-phase flow systems, *J. Heat Transfer ASME*, 87(4), 453-468, 1965.